Deficiency of ribosomal protein S19 during early embryogenesis leads to reduction of erythrocytes in a zebrafish model of Diamond-Blackfan anemia

Tamayo Uechi, Yukari Nakajima, Anirban Chakraborty, Hidetsugu Torihara, Sayomi Higa, Naoya Kenmochi*

Frontier Science Research Center, University of Miyazaki, Miyazaki, 889-1692, Japan.

*Correspondence author:

Dr. Naoya Kenmochi

Frontier Science Research Center

University of Miyazaki

5200 Kihara, Kiyotake, Miyazaki

889-1692, Japan

Tel. +81-985-85-9084

Fax. +81-985-85-9084

Email: kenmochi@med.miyazaki-u.ac.jp

Abstract

Ribosomes are responsible for protein synthesis in all cells. Ribosomal protein S19 (RPS19) is one of the 79 ribosomal proteins in vertebrates. Heterozygous mutations in *RPS19* have been identified in 25% of patients with Diamond-Blackfan anemia (DBA), but the relationship between *RPS19* mutations and the pure red-cell aplasia of DBA is unclear. In this study, we developed an RPS19-deficient zebrafish by knocking down *rps19* using a Morpholino antisense oligo. The RPS19-deficient animals showed a dramatic decrease in blood cells as well as deformities in the head and tail regions at early developmental stages. These phenotypes were rescued by injection of zebrafish *rps19* mRNA, but not by injection of *rps19* mRNAs with mutations that have been identified in DBA patients. Our results indicate that *rps19* is essential for hematopoietic differentiation during early embryogenesis. The effects were specific to *rps19,* but knocking down the genes for three other ribosomal proteins, *rpl35*, *rpl35a,* and *rplp2*, produced similar phenotypes, suggesting that these genes might have a common function in zebrafish erythropoiesis. The RPS19-deficient zebrafish will provide a valuable tool for investigating the molecular mechanisms of DBA development in humans.

Introduction

Diamond–Blackfan anemia (DBA) is characterized by diminished numbers of erythroid progenitors in bone marrow in early infancy. In some cases, patients also show diverse physical abnormalities, such as upper limb malformations, short stature, and kidney dysfunction (1, 2). DNA analysis of a DBA patient with a translocation at 19q13 identified ribosomal protein (RP) S19 as a candidate disease gene for DBA (3). Subsequently, heterozygous mutations in *RPS19* were detected in 25% of 172 patients (4). RPS19 is one of 79 ribosomal proteins, and is expressed in every cell where protein synthesis occurs. It is still unclear how the mutations in such a ubiquitously expressed gene specifically affect erythropoiesis.

Several attempts have been made to address this question, mainly using cell lines. For instance, cells with siRNA-mediated knockdown of the *RPS19* gene proliferate less (5) and have defects in erythroid differentiation similar to those seen in DBA patients (6). Apoptotic changes in progenitor cells have been suggested to be a major factor for anemia development, as evidenced by increased apoptosis in $CD34^+$ cells from DBA patients as well as in siRNA-treated RPS19-deficient cells (7). Others have suggested that cell cycle arrest at G0/G1, not apoptosis, is more critical for the development of anemia (8). Regardless of the mechanism involved, the question remains how a lack of RPS19 protein disturbs the proliferation of erythroid precursors.

Recently, defects in ribosome biogenesis have been proposed to be important in DBA pathogenesis. *RPS19* mutations result in the accumulation of premature

ribosomal RNAs (rRNAs) in patient-derived cells and in RPS19-deficient cell lines (9, 10). When transfected into human cell lines, RPS19 proteins with the mutations seen in DBA patients fail to associate with ribosomes (11). Moreover, mutations in two other RP genes, *RPS24* and *RPS17*, have also been identified in a small but significant number of DBA patients (12, 13), suggesting that changes in ribosomal function could be responsible for the defective erythropoiesis in DBA.

In vertebrates, ribosomes are composed of four rRNA species and 79 different proteins (14-16). Although RPs are essential for the assembly of ribosomes, not much is known about their role, if any, during translation. Therefore, elucidating the currently unknown functions of RPs should provide significant insight into the pathogenesis of DBA and other ribosome-associated diseases. To date, only a single animal model, *Rps19*-knockout mice, has been developed to explore the role of *RPS19* in DBA (17). However, *Rps19*-heterozygous mice in this model system display no abnormalities in any organ, including the hematopoietic system, whereas the null mice die embryonically. Here we report the development of *rps19*-knockdown zebrafish that show marked reduction in erythrocyte numbers during embryogenesis.

Results

Phenotypes of *rps19*-knockdown embryos

Mutations in universally expressed genes, such as RP genes, are generally assumed to result in systemic abnormalities. However, in our previous study, embryos injected with

Morpholino antisense oligos (MOs) against 20 different RP genes showed specific phenotypes depending on the RP gene targeted (18). This suggests that each RP has a specific, although unknown, function during early development in zebrafish. To investigate the specific role of the *RPS19* gene in erythropoiesis, we knocked down the zebrafish ortholog (*rps19*) using MOs and analyzed the effect on the synthesis of blood cells.

The coding region of *rps19* shares 78% nucleotide and 88% amino acid identity with its human ortholog. Although gene duplication is common in zebrafish, available information from public databases suggests that *rps19* exists as a single copy in the genome. We targeted this gene using an MO aimed at its translation initiation site. Following injection of this MO at the one-cell stage, we compared the morphological features of the morphants with wild-type siblings at about 24 hours postfertilization (hpf). At this stage, pigmentation in the retina begins to appear and somitogenesis is completed. The *rps19* morphants showed incomplete brain subdivisions and a ventrally bent tail (Fig. 1). We also observed other phenotypes commonly associated with RP morphants (18), such as an incomplete yolk sac extension and a rough surface appearance. The embryos injected with a control MO did not display any morphological changes. All the *rps19* morphants died by 10 days postfertilization.

Reduced red blood cell synthesis in *rps19*-knockdown embryos

Blood circulation in wild-type zebrafish is easily visible in the posterior cardinal vein and the common cardial vein by 26 hpf. However, the process was delayed by 2 to 3

hours in the *rps19* morphants. Therefore, we compared the circulation pattern of the morphants at 29 hpf with that of wild-type embryos at 26 hpf. *Rps19* morphants showed an obvious reduction in the circulating blood cells compared to the control embryos (Supplementary Material, Fig. S1-S4), and this reduction continued even at later stages of development.

When observed at 48 hpf, the heart in normal embryos appeared red-colored due to a high density of blood cells; however, it was almost transparent in *rps19* morphants, indicating a decreased number of blood cells (Fig. 2B, arrow). To further confirm this reduction, we performed hemoglobin staining on the embryos. As expected, the hemoglobin staining observed in the cardial vein (Fig. 2C, light gray dots) was markedly decreased in the morphants. To investigate if this reduction in blood cells was common in RP deficient embryos, we carried out hemoglobin staining of 19 additional RP morphants. All the 19 RP morphants showed varying degrees of morphological abnormalities, however, there was no correlation between the staining intensity and severity of the associated morphological defects (described below). This suggests that defective blood cell production is a consequence of a specific RP deficiency.

Primitive erythropoiesis defects in *rps19* morphants

To determine the onset of defective erythropoiesis, we analyzed the expression pattern of *gata1*, an early erythroid gene, by whole mount *in situ* hybridization. Because the initiation of circulation was slow in the morphants due to the developmental delay, we examined *gata1* expression at different developmental stages (23-27 hpf) in wild-type

and MO-injected embryos. The *gata1* expression in the intermediate cell mass (ICM) peaked around 24 hpf in the wild-type embryos, whereas it peaked around 26 hpf in the morphants (Fig. 3A, b and e). However, when compared to *gata1* mRNA levels at appropriate developmental stages, the expression level of *gata1* mRNA was not significantly different between the wild-type embryos and the morphants until the onset of circulation (Fig. 3A, a and d, b and e). In contrast, when erythroblasts matured into erythrocytes during circulation (19), *gata1* mRNA was detected in the yolk region of wild-type embryos, but not in the morphants, although their *gata1* expression patterns at ICM were similar (Fig. 3A, c and f).

To further confirm the specificity of the erythroid defects caused by *rps19* deficiency, we examined the expression of vascular and myeloid lineage genes. The expression of *tie-1* (Fig. 3B) and *fli-1a* (data not shown) during vasculogenesis was similar in the wild-type and MO-injected embryos. Similarly, semi-quantitative RT-PCR of other myeloid genes, including *pu.1*, *l-plastin*, and *mpo*, did not show any significant difference in the transcript levels at 24 hpf (Fig. 3C). To confirm the localization of these genes, we carried out *in situ* hybridization and found no obvious differences in the expression patterns between the wild-type embryos and the morphants (Supplementary Material, Fig. S5). Even at 48 hpf, a stage when significant reduction of erythrocytes occurred in the morphants as judged by hemoglobin staining (Fig. 2D), the expression level of *l-plastin* and *mpo* was similar in both types of embryos (data not shown). These data indicate that maturation and proliferation of the erythroid lineage is the main defect of the morphants.

Phenotypic rescue in the morphants by *rps19* mRNA synthesized *in vitro*

Since the reduced blood cell phenotype was specific to RPS19 deficiency, we examined whether a synthesized *rps19* mRNA could rescue this phenotype in embryos. For this, we incorporated a five-base change into the MO-target site of the *rps19* mRNA to prevent *in vivo* binding of the MO to the synthesized mRNA (Fig. 4A). Co-injection of this mRNA (1.0 μM) with the rps19 MO (60 μM) resulted in almost complete recovery of blood cells, as observed by hemoglobin staining and observation of gross morphology (Fig. 4B). These results confirm that the decreased blood cell synthesis is directly related to the RPS19 deficiency in zebrafish.

Several types of mutations, including allelic loss, point mutations, insertions, and deletions, have been identified in the *RPS19* gene of DBA patients (4, 20). Among these, a missense mutation at the 62nd amino acid and a nonsense mutation at the 94th amino acid, both in exon 4 of the gene, occur at high frequency. We assessed whether mRNAs containing these patient-type mutations could rescue the *rps19* phenotype (Fig. 4A). However, when we injected these two mutated mRNAs at a 1.0 μM concentration, which is sufficient for rescue by nonmutated mRNA, the embryos displayed more severe developmental defects than the *rps19* morphants (data not shown). Even in wild-type embryos, injection of these mRNAs at the same concentration resulted in morphological abnormalities (data not shown). Injection of these mRNAs at a lower concentration (0.5 μM) did not induce any additional deformities, but also did not rescue the blood cell production and other associated phenotypes of the knockdown (Fig.

4C). These results indicate that the *rps19* mutations seen in patients remove the normal function of the RPS19 protein and therefore render them unable to rescue red blood cell synthesis in the zebrafish displaying defective erythropoiesis.

Reduced red blood cell synthesis in other RP morphants

Recently, it was proposed that the pathogenesis of DBA might be linked to functional changes in the translational machinery due to defective RPs (21, 22). We therefore investigated the possibility that RP genes other than *RPS19* could contribute to the onset of DBA.

We examined the circulation pattern and the red blood cell density in 20 different RP morphants at various stages of development (26-48 hpf) by using live video imaging and hemoglobin staining. Most of the RP morphants displayed an initial delay in circulation compared to the wild-type embryos, which may be due to a general effect of RP deficiency. Therefore, we focused on whether these initial circulatory defects recovered during later stages of development. We categorized the defects into three different groups: severe, moderate, and almost normal. Our observations revealed that the circulatory defects and blood cell reduction were consistent in three RP morphants in addition to *rps19*: *rpl35*, *rpl35a*, and *rplp2* (Table 1). Although the morphological phenotypes differed among them, the blood cell defects were similar to those of the *rps19* morphants, as indicated by a dramatic decrease in hemoglobin staining (Fig. 5). Thus, these four RP genes might have a common function in zebrafish erythropoiesis.

Discussion

RPS19-deficient zebrafish as a DBA model

Since the first report of DBA in 1938 (23), not much has been learned about its pathogenic mechanisms. Although the *RPS19* gene was identified as a candidate disease gene in 1999 (3), we still have not been able to understand this disease completely. Recent studies of DBA and other inherited bone marrow (BM)-related diseases indicate a possible connection between the translational machinery and BM defects (24, 25). For instance, the *SBDS* gene, predicted to have a role in ribosome biogenesis, is mutated in Shwachman-Diamond Syndrome, a disease characterized by exocrine pancreatic insufficiency, BM failure, and other somatic abnormalities (26, 27). Similarly in dyskeratosis congenita and cartilage-hair hypoplasia, mutations have been identified in the genes that encode proteins involved in ribosome biogenesis (28, 29). However, like DBA, there is currently no direct evidence to prove the relationship between the mutations in these genes and the resultant clinical features of the diseases. Although the molecular mechanisms of pathogenesis are not understood in these BM disorders, the ribosome seems to be a common link between them. Therefore, elucidating the underlying mechanism in DBA may bring new insights into other ribosome-associated diseases as well.

Studies using cell lines and cells derived from DBA patients demonstrated

that changes in basic cellular functions, such as apoptosis and cell cycle arrest, contribute to DBA development (7, 8). However, these observations, although important, focused on the erythroid lineages, and changes in other tissues may have been overlooked. To investigate the mechanisms underlying the erythroid specificity of *RPS19* depletion, studies in animal models are necessary. A previous attempt to use *Rps19*-knockout mice was unsuccessful because the complete loss of the gene resulted in embryonic lethality, and loss of a single allele did not produce any unusual phenotype (17, 30). Although it is not clear why the *Rps19* heterozygous mice developed normally, given that DBA patients have heterozygous mutations, it seems that *Rps19* knockout mice are not a suitable animal model for DBA. As an alternative approach, we knocked down *rps19* in zebrafish. In this study, we successfully demonstrated that the loss of *rps19* function in zebrafish recapitulates the DBA phenotype of a severe decrease in the production of erythroid cells. However, early erythropoiesis was not disrupted, as suggested by the normal expression of *gata1* (Fig.3). In contrast, the level of mature erythrocytes was significantly lower in the morphants. This may indicate the existence of an unknown mechanism causing pure red-cell anemia. There are several advantages to using zebrafish that make this model appropriate for studying the molecular mechanism of DBA. First, the morphology and the maturation process of erythroid cells closely resemble those in mammals. Second, the blood cells in the early stages of development consist mainly of erythroid progenitors, which are the primary targets in DBA, making the analysis of the hematopoietic system easier. Third, the embryos can survive for several days even in the absence of blood cells, and hence are suitable for

anemia research (31).

Effects of mutated S19 proteins on embryogenesis

In this zebrafish system, the blood cell reduction was easily rescued by *rps19* mRNA, but not by mRNAs with DBA patient–type mutations. Interestingly, these mutated mRNAs, when overexpressed, led to severe phenotypes different from those seen in *rps19* morphants. A previous *in vitro* study demonstrated that mutated S19 proteins failed to assemble into the ribosomes (11). It is conceivable that the defective ribosome biogenesis may have deleterious effects on embryogenesis. Alternatively, mutated S19 could alter the translational efficiency in a mature ribosome, leading to abnormal phenotypes. Although the exact mechanism is still unclear, it is likely that expression of a defective RPS19 protein affects morphogenesis in zebrafish in a way that differs from the absence of RPS19 due to MO knockdown.

Other RP genes potentially involved in hematopoiesis

Many RPs are believed to have additional functions besides their role in ribosomes (32, 33). Initially, the loss of such an extraribosomal function of RPS19 was assumed to be the cause of the pure red-cell aplasia in DBA (3). Subsequent studies, however, suggested that the ribosome itself has a role in this disease. If so, involvement of other RP genes in DBA seems plausible. Interestingly, mutations in *RPS24* and *RPS17* have been identified in some DBA patients who do not have any mutation in *RPS19* (12, 13). Therefore, some RP genes may have shared functions that are important for

hematopoiesis. In this study, the morphants for *rpl35*, *rpl35a*, and *rplp2* genes also displayed a severe reduction in blood cell production. We assume that, like *rps19* morphants, the erythropoietic system is impaired in these morphants, suggesting that these RPs have a common role in hematopoiesis. Recently, mutations in *RPL35A* were reported in DBA patients (34), indicating the usefulness of our data for screening other DBA candidate genes.

Ribosome defects and human diseases

In *Drosophila,* haploinsufficiency of any RP gene leads to the *Minute* mutant, which displays thin bristles, poor fertility, and an overall developmental delay (35, 36). Such phenotypes are believed to be a consequence of decreased translational efficiency due to a reduction of fully functional ribosomes. However, *Ts* and *Bst* mutants in mice (37, 38) and DBA in humans, which are strongly linked to mutations in RP genes, display tissue-specific phenotypes. It is conceivable that loss of function of a specific RP may not be critical for all cell types. Accordingly, a lower *RPS19* gene dosage may not have the same effect on other cells. In other words, mutations in *RPS19* may lead to serious defects in the erythroid lineage but not in other cell lineages. Recently, it was reported that the yeast ribosomes include a subset of paralogous RPs, and specific combinations of RPs are required for translating specific mRNAs (39). Thus, in higher organisms, such functionally specific RPs may impart organ-specific translational preferences to ribosomes, and depletion of an RP may lead to selective effects in a particular organ. Based on this assumption, we hypothesize that, in DBA, the mutations in the *RPS19*

gene affect the translational efficiency of mRNAs essential for erythroblast differentiation. The RSP19-deficient zebrafish model developed in this study could be a valuable tool to explore this possibility and shed light on the relationship between RPS19 mutations and erythroid cell susceptibility in DBA.

Materials and Methods

Morpholino microinjections

MOs were obtained from Gene Tools, LLC (Philomath, OR). The MOs were injected into one-cell-stage embryos at a concentration of 0.5 μg/μl. The sequences of the MOs were rps19 MO, 5'-CACTGTTACACCACCTGGCATCTTG, and control MO, 5'-CACTcTTAgACgCACCTGcCATgTTG (bases complementary to the start codon are underlined and mispaired bases are shown in lower case). The sequences of the 19 other RP MOs can be found in our database (http://zebrafish.med.miyazaki-u.ac.jp). These MOs were injected into embryos at the optimal concentrations indicated elsewhere (18).

Whole mount *in situ* hybridizations

Digoxigenin-labeled antisense riboprobes were transcribed from a linearized plasmid containing *gata1* and a PCR-based template containing *tie-1* using DIG RNA labeling Mix and T7 RNA polymerase (Roche). The template for the *tie-1* probe was generated by PCR using the forward primer 5'-CTGGCCCTCTTTTACATTCG and reverse primer 5'-TAATACGACTCACTATAGGGACTAGGCAGTCTTCCCATGGTTT.

Semi-quantitative RT-PCR

Total RNA was isolated from wild-type and MO-injected embryos using TRIzol reagent (Invitrogen). Semi-quantitative RT-PCR was performed with 0.5 μg total RNA using a OneStep RT-PCR kit (Qiagen). The primer pairs for each gene were as follows: *pu.1*, 5'-CAGAGCTACAAAGCGTGCAG, and 5'-GCAGAAGGTCAAGCAGGAAC; *l-plastin*, 5'-GGCATACGGGAGAAAGATGA and 5'-ATGTTGCTGCCCAGTTTAGG; *mpo*, 5'-AGGGCGTGACCATGCTATAC and 5'-CGGTGTTGTCGCAGATTATG; *beta-actin*, 5'-GCCCATCTATGAGGGTTACG and 5'-GCAAGATTCCATACCCAGGA.

mRNA synthesis for rescue experiments

Full-length *rps19* (GenBank accession no. NM_200750) was amplified by PCR using the forward primer 5'-GCAAGATGCCAGGTGGTGT and the reverse primer 5'-TTATTTTACACTTTCTTGCTTGCAG and cloned into a TA vector (Promega, Madison, WI). Using this TA vector as a template, we generated the cDNA for 'modified *rps19*', which included a silent five-base change around the MO binding site. We used this as a template to synthesize 'missense *rps19*' and 'nonsense *rps19*' mRNAs, corresponding to two mutations found in DBA patients. These cDNAs were then digested by *EcoRI* and cloned into a pCS2+ vector (provided by Dr. Kunio Inoue, Kobe university, Japan) for *in vitro* transcription. Capped mRNAs were synthesized from 1 μg of the linearized template by SP6 RNA polymerase using an mMessage mMachine kit **(**Ambion**,** Austin, TX**).**

Observation of blood cell circulation and hemoglobin staining

The embryos were grown at 28.5℃ and the circulating blood cells in the posterior cardinal vein and the common cardial vein were recorded at 26 and 29 hpf by live video imaging using CCD camera (DP70, Olympus) attached to a stereoscopic microscope (SZX12, Olympus). To examine the density of red blood cells around the cardial vein at 32-48 hpf, we carried out hemoglobin staining using *o*-dianisidine as previously described (40). We divided the RP morphants into three groups depending on the extent of recovery of the blood cell density and circulation pattern at later stages of development.

Acknowledgement

We thank Dr. Kunio Inoue for kindly providing the pCS2+ vector; Dr. Noriyoshi Sakai and Dr. Minori Shinya for technical advice; Dr. Kinta Hatakeyama, Dr. Yujiro Asada, and Ms. Ritsuko Sotomura for useful suggestions; and Dr. Maki Yoshihama for useful discussions.

Conflict of interest statement

None declared.

Funding

This work was supported by Grants-in-Aid (20790734, 20659044, 1806457) from the

Ministry of Education, Culture, Sports, Science, and Technology (MEXT) and Japan Society for the Promotion of Science (JSPS), and funds from The Life Science Foundation of Japan and The Naito Foundation. A.C. is a research fellow of JSPS (P06457).

References

1. Ball, S.E., McGuckin, C.P., Jenkins, G., Gordon-Smith, E.C. (1996) Diamond-Blackfan anaemia in the U.K.: analysis of 80 cases from a 20-year birth cohort. *Brit. J. Haematol*., **94**, 645-653.

2. Lipton, J.M., Atsidaftos, E., Zyskind, I., Vlachos, A. (2006) Improving clinical care and elucidating the pathophysiology of Diamond Blackfan anemia: an update from the Diamond Blackfan Anemia Registry. *Pediart. Blood Cancer*, **46**, 558-564.

3. Draptchinskaia, N., Gustavsson, P., Andersson, B., Pettersson, M., Willig, T.N., Dianzani, I., Ball, S., Tchernia, G., Klar, J., Matsson, H. *et al*. (1999) The gene encoding ribosomal protein S19 is mutated in Diamond-Blackfan anaemia. *Nat. Genet*., **21**, 169-175.

4. Willig, T.N., Draptchinskaia, N., Dianzani, I., Ball, S., Niemeyer, C., Ramenghi, U., Orfali, K., Gustavsson, P., Garelli, E., Brusco, A. *et al*. (1999) Mutations in ribosomal protein S19 gene and diamond blackfan anemia: wide variations in phenotypic expression. *Blood*, **94**, 4294-4306.

5. Miyake, K., Flygare, J., Kiefer, T., Utsugisawa, T., Richter, J., Ma, Z., Wiznerowicz, M., Trono, D., Karlsson, S. (2005) Development of cellular models for ribosomal protein S19 (RPS19)-deficient diamond-blackfan anemia using inducible expression of siRNA against RPS19. *Mol. Ther*., **11**, 627-637.

6. Flygare, J., Kiefer, T., Miyake, K., Utsugisawa, T., Hamaguchi, I., Da Costa, L., Richter, J., Davey, E.J., Matsson, H., Dahl, N. *et al*. (2005) Deficiency of ribosomal protein S19 in $CD34^+$ cells generated by siRNA blocks erythroid development and mimics defects seen in Diamond-Blackfan anemia. *Blood*, **105**, 4627-4634.

7. Miyake, K., Utsugisawa, T., Flygare, J., Kiefer, T., Hamaguchi, I., Richter, J., Karlsson, S. (2008) Ribosomal protein S19 deficiency leads to reduced proliferation and increased apoptosis but does not affect terminal erythroid differentiation in a cell line model of Diamond-Blackfan anemia. *Stem Cells*, **26**, 323-329.

8. Kuramitsu, M., Hamaguchi, I., Takuo, M., Masumi, A., Momose, H., Takizawa, K., Mochizuki, M., Naito, S., Yamaguchi, K. (2008) Deficient RPS19 protein production induces cell cycle arrest in erythroid progenitor cells. *Br. J. Haematol*., **140**, 348-359.

9. Flygare, J., Aspesi, A., Bailey, J.C., Miyake, K., Caffrey, J.M., Karlsson, S., Ellis, S.R. (2007) Human *RPS19*, the gene mutated in Diamond-Blackfan anemia, encodes a ribosomal protein required for the maturation of 40S ribosomal subunits. *Blood*, **109**, 980-986.

10. Choesmel, V., Bacqueville, D., Rouquette, J., Noaillac-Depeyre, J., Fribourg, S., Crétien, A., Leblanc, T., Tchemia, G., Da Costa, L., Gleizes, P.E. (2007) Impaired ribosome biogenesis in Diamond-Blackfan anemia. *Blood*, **109**, 1275-1283.

11. Angelini, M., Cannata, S., Mercaldo, V., Gibello, L., Santoro, C., Dianzani, I., Loreni, F. (2007) Missense mutations associated with Diamond-Blackfan anemia affect the assembly of ribosomal protein S19 into the ribosome. *Hum. Mol. Genet*., **16**, 1720-1727.

12. Gazda, H.T., Grabowska, A., Merida-Long, L.B., Latawiec, E., Schneider, H.E., Lipton, J.M., Vlachos, A., Atsidaftos, E., Ball, S.E., Orfali, K.A. *et al*. (2006)

Ribosomal protein S24 gene is mutated in Diamond-Blackfan anemia. *Am. J. Hum. Genet*., **79**, 1110-1118.

13. Cmejla, R., Cmejlova, J., Handrkova, H., Petrak, J., Pospisilova, D. (2007) Ribosomal protein S17 gene (RPS17) is mutated in Diamond-Blackfan anemia. *Hum. Mutat*., **28**, 1178-1182.

14. Wool, I.G. (1979) The structure and function of eukaryotic ribosomes. *Annu. Rev. Biochem*., **48**, 719-754.

15. Yoshihama, M., Uechi, T., Asakawa, S., Kawasaki, K., Kato, S., Higa, S., Maeda, N., Minoshima, S., Tanaka, T., Shimizu, N., Kenmochi, N. (2002) The human ribosomal protein genes: sequencing and comparative analysis of 73 genes. *Genome Res.*, **12**, 379-390.

16. Nakao, A., Yoshihama, M., Kenmochi, N. (2004) RPG: the Ribosomal Protein Gene database. *Nucleic Acids Res*., **32**(Database issue), D168-170.

17. Matsson, H., Davey, E.J., Draptchinskaia, N., Hamaguchi, I., Ooka, A., Levéen, P., Forsberg, E., Karlsson, S., Dahl, N. (2004) Targeted disruption of the ribosomal protein S19 gene is lethal prior to implantation. *Mol. Cell. Biol*., **24**, 4032-4037.

18. Uechi, T., Nakajima, Y., Nakao, A., Torihara, H., Chakraborty, A., Inoue, K., Kenmochi, N. (2006) Ribosomal protein gene knockdown causes developmental defects in zebrafish. *PLoS ONE*, **1**, e37

19. Herbomel, P., Thisse, B., Thisse, C. (1999) Ontology and behaviour of early macrophages in the zebrafish embryo. Development, **126**, 3735-3745.

20. Orfali, K.A., Ohene-Abuakwa, Y., Ball, S.E. (2004) Diamond Blackfan anaemia in the UK: clinical and genetic heterogeneity. *Brit. J. Haematol*., **125**, 243-252.

21. Gazda, H.T., Kho, A.T., Sanoudou, D., Zaucha, J.M., Kohane, I.S., Sieff, C.A., Beggs, A.H. (2006) Defective ribosomal protein gene expression alters transcription, translation, apoptosis, and oncogenic pathways in Diamond-Blackfan anemia. *Stem Cells,* **24**, 2034-2044.

22. Cmejlova, J., Dolezalova, L., Pospisilova, D., Petrtylova, K., Petrak, J., Cmejla, R. (2006) Translational efficiency in patients with Diamond-Blackfan anemia. *Haematologica*, **91**, 1456-1464.

23. Diamond, L.K., Blackfan, K.D. (1938) Hypoplastic anemia. *Am. J. Dis. Child*., **56**, 464-467.

24. Liu, J.M., Ellis, S.R. (2006) Ribosomes and marrow failure: coincidental association or molecular paradigm?, *Blood*, **107**, 4583-4588.

25. Dokal, I., Vulliamy, T. (2008) Inherited aplastic anaemias/bone marrow failure syndromes. *Blood Rev*., **22**, 141-153.

26. Boocock, G.R., Morrison, J.A., Popovic, M., Richards, N., Ellis, L., Durie, P.R., Rommens, J.M. (2003) Mutations in *SBDS* are associated with Shwachman-Diamond syndrome. *Nat. Genet*., **33**, 97-101.

27. Menne, T.F., Goyenechea, B., Sánchez-Puig, N., Wong, C.C., Tonkin, L.M., Ancliff, P.J., Brost, R.L., Costanzo, M., Boone, C., Warren, A.J. (2007) The Shwachman-Bodian-Diamond syndrome protein mediates translational activation of ribosomes in yeast. *Nat. Genet*., **39**, 486-495.

28. Heiss, N.S., Knight, S.W., Vulliamy, T.J., Klauck, S.M., Wiemann, S., Mason, P.J., Poustka, A., Dokal, I. (1998) X-linked dyskeratosis congenita is caused by mutations in a highly conserved gene with putative nucleolar functions. *Nat. Genet*., **19**, 32-38.

29. Ridanpää, M., van Eenennaam, H., Pelin, K., Chadwick, R., Johnson, C., Yuan, B., vanVenrooij, W., Pruijn, G., Salmela, R., Rockas, S., *et al*. (2001) Mutations in the RNA component of RNase MRP cause a pleiotropic human disease, cartilage-hair hypoplasia. *Cell*, **26**, 195-203.

30. Matsson, H., Davey, E.J., Fröjmark, A.S., Miyake, K., Utsugisawa, T., Flygare, J., Zahou, E., Byman, I., Landin, B., Ronquist, G., Karlsson, S., Dahl, N. (2006) Erythropoiesis in the *Rps19* disrupted mouse: Analysis of erythropoietin response and biochemical markers for Diamond-Blackfan anemia. *Blood Cells Mol. Dis*., **36**, 259-264.

31. North, T.E., Zon, L.I. (2003) Modeling human hematopoietic and cardiovascular diseases in zebrafish. *Dev. Dyn*., **228**, 568-583.

32. Wool, I.G. (1996) Extraribosomal functions of ribosomal proteins. *Trends Biochem. Sci.,* **21**, 164-165.

33. Mazumder, B., Sampath, P., Seshadri, V., Maitra, R.K., DiCorlete, P.E., Fox, P.L. (2003) Regulated release of L13a from the 60S ribosomal subunit as a mechanism of transcript-specific translational control. *Cell*, **115,** 187-198.

34. Farrar, J.E., Nater, M., Caywood, E., McDevitt, M.A., Kowalski, J., Takemoto, C.M., Talbot, C.C. Jr., Meltzer, P., Esposito, D., Beggs, A.H. *et al.* (2008) Abnormalities of the large ribosomal subunit protein, Rpl35A, in diamond-blackfan anemia. *Blood*, in press.

35. Lambertsson, A. (1998) The *minute* genes in *Drosophila* and their molecular functions. *Adv. Genet*., **38**, 69-134.

36. Marygold, S.J., Roote, J., Reuter, G., Lambertsson, A., Ashburner, M., Millburn, G.H., Harrison, P.M., Yu, Z., Kenmochi, N., Kaufman, T.C. *et al*. (2007) The ribosomal protein genes and *Minute* loci of *Drosophila melanogaster*. *Genome Biol*., **8**, R216.

37. Ishijima, J., Yasui, H., Morishima, M., Shiroishi, T. (1998) Dominant lethality of the mouse skeletal mutation tail-short (*Ts*) is determined by the *Ts* allele from mating partners. *Genomics*, **49**, 341-350.

38. Oliver, E.R., Saunders, T.L., Tarlé, S.A., Glaser, T. (2004) Ribosomal protein L24 defect in belly spot and tail (*Bst*), a mouse *Minute*. *Development*, **131**, 3907-3920.

39. Komili, S., Farny, N.G., Roth, F.P., Silver, P.A. (2007) Functional specificity among ribosomal proteins regulates gene expression. *Cell*, **131**, 557-571.

40. Detrich, H.W. 3rd, Kieran, M.W., Chan, F.Y., Barone, L.M., Yee, K., Rundstadler, J.A., Pratt, S., Ransom, D., Zon, L.I. (1995) Intraembryonic hematopoietic cell migration during vertebrate development. *Proc. Natl. Acad. Sci. U. S. A.*, **7**, 10713-10717.

Legends to Figures

Figure 1. Morphological changes in *rps19*-knockdown embryos.

Lateral views of the head and trunk region in wild types (A and B) and morphants (C-F) at 25 hpf. The brain of the *rps19* morphant has improper subdivisions (dotted curve) and a smaller otic capsule (arrow) (C) than the wild-type embryo (A). The body trunks of the morphants show a downward bend in the tail and a thin yolk sac extension (solid line; D). These deformities are not seen in embryos injected with the control MO (E and F). tel, telencephalon; ot, optic tectum; mhb, midbrain-hindbrain-boundary; oc, otic capsule. Scale bar, 200μm.

Figure 2. Drastic reduction of blood cells in the *rps19* morphants.

Lateral views of wild-type (A) and MO-injected embryos (B) at 48 hpf. The heart of the *rps19* morphant (arrow in B) is almost transparent because it has fewer erythrocytes than the wild type. The cardial vein region in the yolk sac is shown in wild-type zebrafish (C) and *rps19* morphants (D). Wild-type embryos contain a high density of blood cells (light gray dots in C), whereas the number of red blood cells is drastically reduced in red blood cells in the *rps19* morphants, as indicated by the absence of hemoglobin-stained cells.

Figure 3. Specific reduction in the levels of erythropoietic marker genes.

(A) Whole mount *in situ* hybridization assay for *gata1* at different developmental stages. The expression pattern of *gata1* in ICM displays no significant difference until circulation starts (a and d, b and e). The *gata1*-expressing circulating cells are detected in the yolk region of wild-type embryos (arrows), but not in that of the morphants (c and f). (B) Whole mount *in situ* hybridization assay for *tie-1*. Although the morphants display a smaller body, the expression pattern of *tie-1* is same as in the wild type. (C) Semi-quantitative RT-PCR for *pu.1*, *l-plastin*, and *mpo* genes. RNAs were prepared from the embryos at 24 hpf. Beta-actin was used as an internal control. WT, wild type; MO, *rps19* morphant. Scale bars, 200 μm.

Figure 4. Rescue of morphological and anemia-like phenotypes by *rps19* mRNA.

(A) Schematic representation of the injected *rps19* mRNAs. In ‘WT rps19’, four codons

(start, stop, and two commonly mutated in the patients) are shown with their corresponding amino acid numbers. The ‘modified rps19’ includes silent mutations (vertical white lines) around the start codon that prevent the binding of the Morpholino (MO; gray line on the top) to the mRNAs. ‘Missense rps19’ and ‘nonsense rps19’ mRNAs also include, respectively, an amino acid change of arginine to tryptophan at the 63rd amino acid and a premature stop codon instead of valine at the 95th amino acid. (B) Morphological observations and hemoglobin staining of embryos coinjected with MO-resistant *rps19* mRNA and rps19 MO. The MO-injected embryos show bent tails, reduced yolk sac extensions (arrows in a), and fewer blood cells (orange dots in d). These phenotypes were rescued by injection of 1.0 μM modified mRNA (b and e), and attained almost the same phenotype as the wild type (c and f). (C) Morphological observations and hemoglobin staining of embryos coinjected with MO-resistant, mutated *rps19* mRNA and rps19 MO. Less of the modified mRNA (0.5 μM) still rescues the *rps19* phenotypes (a and d), whereas the embryos injected with the mutated mRNAs at the same concentration (b, c, e, and f) display abnormal phenotypes similar to those in *rps19* morphants.

Figure 5. Reduction of blood cells in *rpl35*, *rpl35a*, and *rplp2* morphants.

Hemoglobin staining of cardial veins at 48 hpf. Compared to the *rpl36a* morphants (A), a morphant that display a moderate level of blood cell recovery (Table 1), the *rpl35*, *rpl35a*, and *rplp2* morphants (B-D) show a drastic reduction in number of hemoglobin stained blood cells (orange dots).

Table 1. The extent of reduction in red blood cells by RP gene knockdown

	Blood cell circulation		Blood cell density
Phenotypes	Posterior caudal vein	Cardial vein	Hb staining
None	*rps3*	*rps3*	*rps15*
	rps4	*rps8*	*rpl28*
	rpl11	*rpl11*	
	rpl24	*rpl36a*	
	rpl36a		
Moderate	*rps8*	*rps3a*	*rps3a*
	rps15	*rps4*	*rps4*
	rps15a	*rps15*	*rps8*
	rps24	*rps15a*	*rps15a*
	rps29	*rps24*	*rps24*
	rpl6	*rps29*	*rpl6*
	rpl28	*rpl6*	*rpl11*
	rpl35a	*rpl24*	*rpl24*
	rpl38	*rpl28*	*rpl36a*
	rplp0	*rpl38*	*rplp38*
	rplp1	*rplp1*	*rplp0*
Severe	*rps3a*	*rps19*	*rps3*
	rps19	*rpl35*	*rps19*
	rpl35	*rpl35a*	*rps29*
	rplp2	*rplp0*	*rpl35*
		rplp2	*rpl35a*
			rplp1
			rplp2

Fig.1

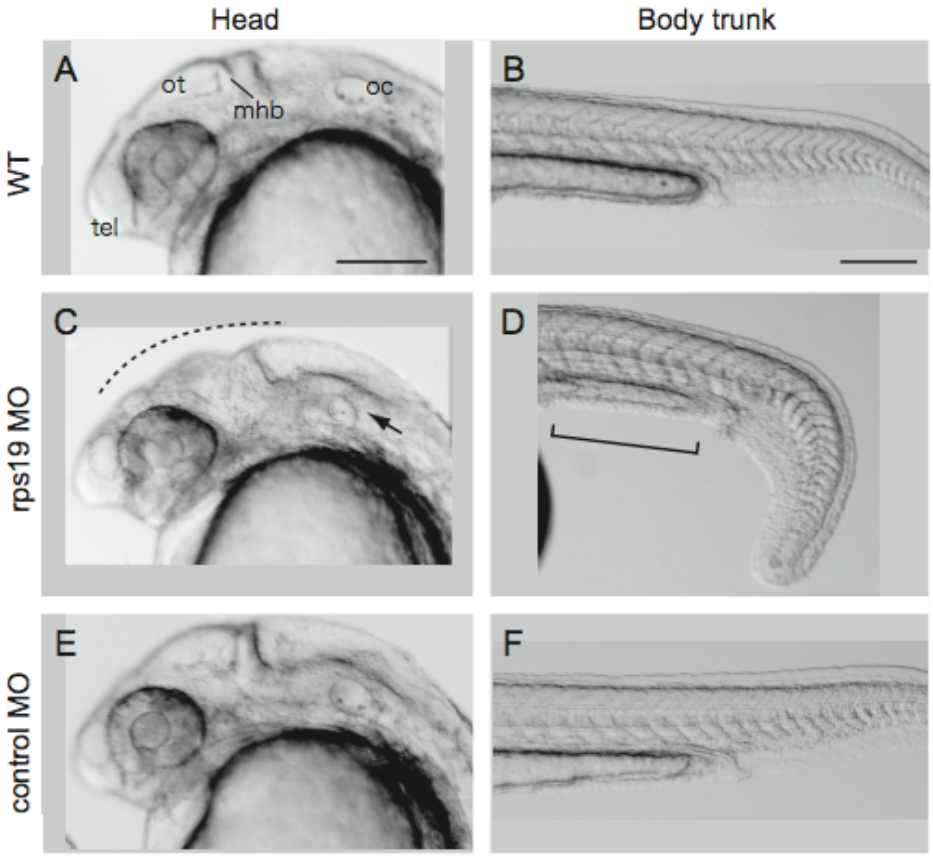

Fig. 2

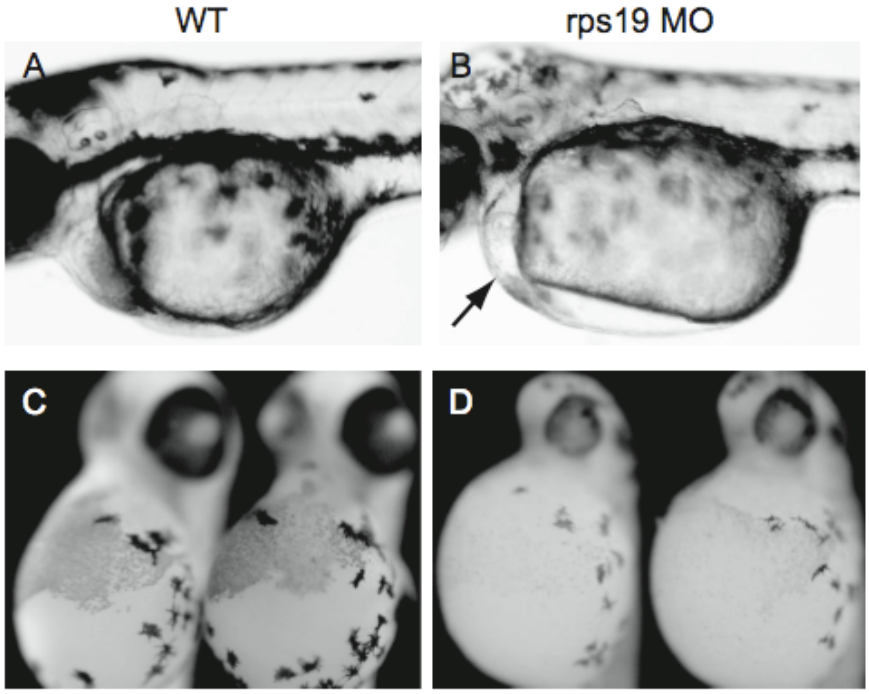

Fig. 3

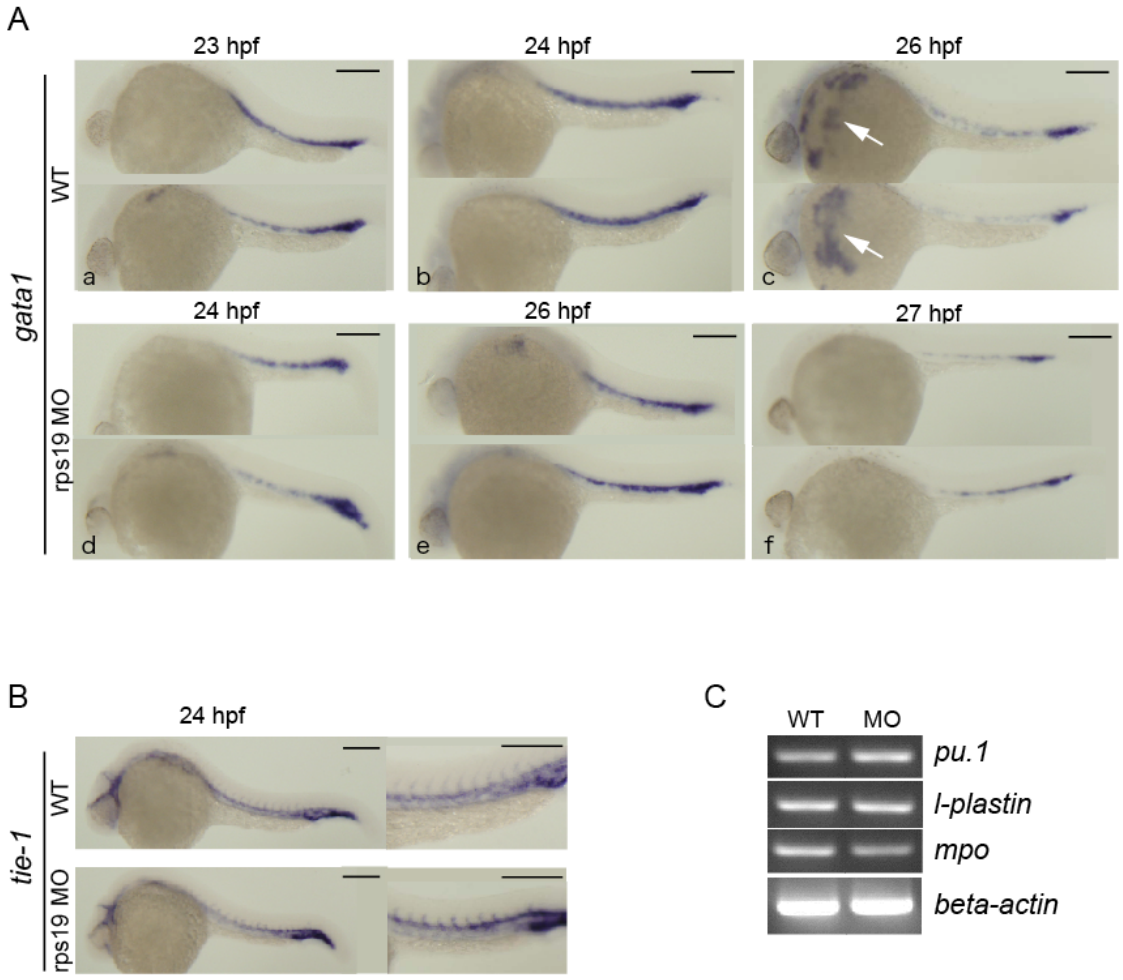
A
23 hpf
24 hpf
26 hpf
gata1
WT
a
b
c
24 hpf
26 hpf
27 hpf
rps19 MO
d
e
f
B
24 hpf
tie-1
WT
rps19 MO
C
WT
MO
pu.1
l-plastin
mpo
beta-actin

Fig. 4

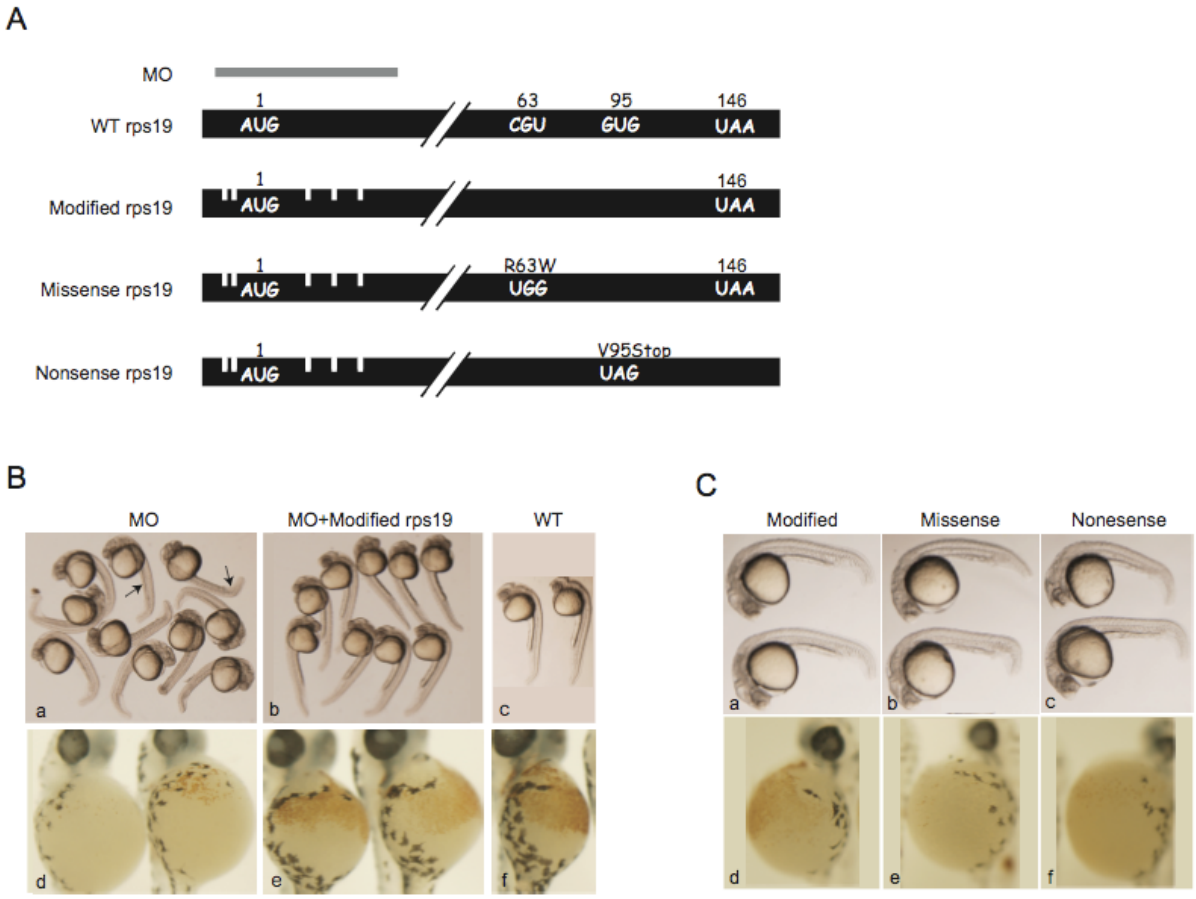
A
MO
WT rps19
1
AUG
63
CGU
95
GUG
146
UAA
Modified rps19
1
AUG
146
UAA
Missense rps19
1
AUG
R63W
UGG
146
UAA
Nonsense rps19
1
AUG
V95Stop
UAG
B
MO
MO+Modified rps19
WT
a
b
c
d
e
f
C
Modified
Missense
Nonesense
a
b
c
d
e
f

Fig. 5

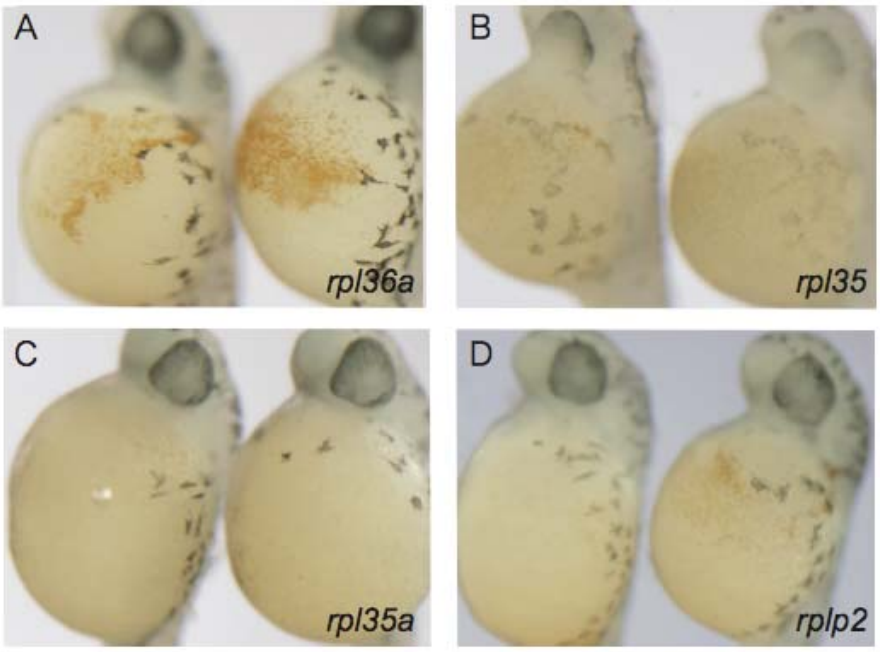

Abbreviations

RP, ribosomal protein; DBA, Diamond-Blackfan Anemia; MO, Morpholino antisense oligo; BM, bone marrow; ICM, intermediate cell mass

Supplementary Data

Figure S1. Circulating blood cells in the common cardial vein of wild-type embryos at 26 hpf.

Figure S2. Circulating blood cells in the common cardial vein of *rps19* morphants at 29 hpf.

Figure S3. Circulating blood cells in the posterior caudal vein of wild-type embryos at 26 hpf.

Figure S4. Circulating blood cells in the posterior caudal vein of *rps19* morphants at 29 hpf.

Figure S5. *In situ* hybridization of myeloid marker genes in wild types and *rps19* morphants at 24 hpf.